PHYSICAL REVIEW D **78,** 083509 (2008)

Dynamics and constraints of the unified dark matter flat cosmologies

Spyros Basilakos[1] and Georgios Lukes-Gerakopoulos[1,2]

[1]*Academy of Athens, Research Center for Astronomy and Applied Mathematics, Soranou Efesiou 4, GR-11527, Athens, GREECE*

[2]*University of Athens, Department of Physics, Section of Astrophysics, Astronomy and Mechanics*

(Received 7 April 2008; revised manuscript received 11 September 2008; published 6 October 2008)

We study the dynamics of the scalar field Friedmann-Lemaitre-Robertson-Walker flat cosmological models within the framework of the *unified dark matter* (UDM) scenario. In this model we find that the main cosmological functions such as the scale factor of the Universe, the scalar field, the Hubble flow, and the equation of state parameter are defined in terms of hyperbolic functions. These analytical solutions can accommodate an accelerated expansion, equivalent to either the *dark energy* or the standard Λ models. Performing a joint likelihood analysis of the recent supernovae type Ia data and the baryonic acoustic oscillations traced by the Sloan Digital Sky Survey galaxies, we place tight constraints on the main cosmological parameters of the UDM cosmological scenario. Finally, we compare the UDM scenario with various dark energy models namely Λ cosmology, parametric dark energy model and variable Chaplygin gas. We find that the UDM scalar field model provides a large and small scale dynamics which are in fair agreement with the predictions by the above dark energy models although there are some differences especially at high redshifts.

DOI: 10.1103/PhysRevD.78.083509 PACS numbers: 98.80.−k, 11.10.Ef

I. INTRODUCTION

The detailed analysis of the available high quality cosmological data (Type Ia supernovae [1,2]; cosmic microwave background (CMB) [3,4], etc.) leads to the conclusion that we live in a flat and accelerating universe. In order to investigate the cosmic history of the observed universe, we have to introduce a general cosmological model which contains cold dark matter to explain the large scale structure clustering and an extra component with negative pressure, the vacuum energy (or in a more general setting the ''dark energy''), to explain the observed accelerated cosmic expansion (Refs. [1–4] and references therein). The nature of the dark energy is one of the most fundamental and difficult problems in physics and cosmology. There are many theoretical speculations regarding the physics of the above exotic dark energy, such as a cosmological constant (vacuum), quintessence, k essence, vector fields, phantom, tachyons, Chaplygin gas, and the list goes on (see [5–18] and references therein).

Such studies are based on the general assumption that the real scalar field ϕ rolls down the potential $V(\phi)$ and therefore it could resemble the dark energy [6,8,11,19–22]. This is very important because scalar fields could provide possible solutions to the cosmological coincidence problem. In this framework, the corresponding stress-energy tensor takes the form of a perfect fluid, with density $\rho_\phi = \dot{\phi}^2/2 + V(\phi)$ and pressure $P_\phi = \dot{\phi}^2/2 - V(\phi)$. From a cosmological point of view, if the scalar field varies slowly with time, so that $\dot{\phi}^2/2V \ll 1$, then $w \equiv P_\phi/\rho_\phi \approx -1$, which means that the scalar field evolves like a vacuum energy. Of course in order to investigate the overall dynamics we need to define the functional form of the potential energy. The simplest example found in the literature is a scalar field with $V(\phi) \propto \phi^2$ (see for review [11,23]) and it has been shown that the time evolution of this scalar field is dominated by oscillations around $\phi = 0$. Of course, the issue of the potential energy has a long history in scalar field cosmology (see [24–28] and references therein) and indeed several parametrizations have been proposed (exponential, power law, hyperbolic, etc.).

The aim of the present work is to investigate the observational consequences of the overall dynamics of a family of flat cosmological models by using a hyperbolic scalar field potential which appears to act both as dark matter and dark energy [29]. To do so, we use the traditional Hamiltonian approach. In fact, the idea to build cosmological models in which the dark energy component is somehow linked with the dark matter is not new in this kind of studies. Recently, alternative approaches to the unification of dark energy and dark matter have been proposed in the framework of the generalized Chaplygin gas [30,31] and in the context of supersymmetry [32].

The structure of the paper is as follows. The basic theoretical elements of the problem are presented in Sec. II by solving analytically [for spatially flat unified dark matter (UDM) scalar field models] the equations of motion. In Sec. III, we present the functional forms of the basic cosmological functions [$a(t)$, $\phi(t)$ and $H(t)$]. In Sec. IV we place constraints on the main parameters of our model by performing a joint likelihood analysis utilizing the SNIa data [2] and the observed baryonic acoustic oscillations (BAO) [33,34]. In particular, we find that the matter density at the present time is $\Omega_m \simeq 0.25$ while the corresponding scalar field is $\phi_0 \simeq 0.42$ in geometrical units (0.084 in Planck units). Section V outlines the evolution of matter perturbations in the UDM model. Also we compare the theoretical predictions provided by the UDM scenario with

those found by three different types of dark energy models namely Λ cosmology, parametric dark energy model, and variable Chaplygin gas. We verify that at late times (after the inflection point) the dynamics of the UDM scalar model is in a good agreement with those predicted by the above dark energy models although there are some differences especially at early epochs: (i) the UDM equation of state parameter takes positive values at large redshifts, (ii) it behaves well with respect to the cosmic coincidence problem, and (iii) before the inflection point the cosmic expansion in the UDM model is much more decelerated than in the other three dark energy models implies that the large scale structures (such as galaxy clusters) are more bound systems with respect to those cosmic structures which produced by the other three dark energy models. Finally, we draw our conclusions in Sec. VI.

II. ANALYTICAL SOLUTIONS IN THE FLAT SCALAR FIELD COSMOLOGY

Within the framework of homogeneous and isotropic scalar field cosmologies it can be proved (see Ref. [35]) that the main cosmological equations (the so-called Friedmann-Lemaitre equations) can be obtained by a Lagrangian formulation:

$$L = -3a\dot{a}^2 + a^3\left[\frac{\dot{\phi}^2}{2} - V(\phi)\right] + 3ka, \tag{1}$$

where $a(t)$ is the scale factor of the universe, $\phi(t)$ is the scalar field, $V(\phi)$ is the potential energy, and $k(=-1, 0, 1)$ is the spatial curvature. Indeed the equations of motion take the following forms [36]:

$$3\left[\left(\frac{\dot{a}}{a}\right)^2 + \frac{k}{a^2}\right] = \frac{\dot{\phi}^2}{2} + V(\phi) \tag{2}$$

$$2\left(\frac{\ddot{a}}{a}\right) + \left(\frac{\dot{a}}{a}\right)^2 + \frac{k}{a^2} = -\frac{\dot{\phi}^2}{2} + V(\phi) \tag{3}$$

and

$$\ddot{\phi} + 3\frac{\dot{a}}{a}\dot{\phi} + V'(\phi) = 0, \tag{4}$$

where the overdot denotes derivatives with respect to time while prime denotes derivatives with respect to ϕ. We would like to stress here that in this work we consider a spatially homogeneous scalar field ϕ, ignoring the possible coupling to other fields and quantum-mechanical effects. On the other hand, introducing in the global dynamics a new degree of freedom, in a form of the scalar field ϕ, it is possible to make the vacuum energy a function of time (see [20,37,38]). Note of course that the geometry of the spacetime is described by the Friedmann-Lemaitre-Robertson-Walker (FLRW) line element.

In order to study the above system of differential equations we need to define explicitly the functional form of the scalar field potential energy, $V(\phi)$, which is not an easy task to do. Indeed, in the literature, due to the unknown nature of the dark energy, there are many forms of potentials proposed by several authors (for a review see [10,16,39]) which describe differently the physics of the scalar field. It is worth pointing out that for some special cases analytical solutions have been found (Refs. [25–28,40–42] and references therein). As an example, if the potential $V(\phi)$ is modeled as a power law ϕ^n, then the energy density of the scalar field evolves like $\rho_\phi \propto a^{-6n/(n+2)}$ which means that, for $n = 2$ or $n = 4$ the corresponding energy density behaves either like non relativistic or relativistic matter. In this work, we have used a functional form of $V(\phi)$ (see [43]) for which we solve the previous dynamical problem analytically. This potential corresponds to the so called *Unified Dark Matter* (hereafter UDM) scenario [28,29,44]:

$$V(\phi) = c_1\cosh^2(\mathcal{D}\phi) + c_2 \qquad \mathcal{D}, c_1, c_2 \in \Re. \tag{5}$$

Following the Bertacca *et al.* [29] nomenclature, the real constants in Eq. (5) are selected such as $c_1 = c_2 > 0$. As expected there is one minimum at the point $\phi = 0$, which reads

$$V_{\min} = V(0) = c_1 + c_2. \tag{6}$$

We would like to point out that as long as the scalar field is taking negative and large values the UDM model has the attractive feature due to $V(\phi) \propto e^{-2\mathcal{D}\phi}$ [24]. This property simply says that the energy density in ϕ tracks [42] the radiation (matter) component. In fact the UDM potential was designed to mimic both the dark matter and the dark energy. Indeed, performing a Taylor expansion to the potential around its minimum we get

$$V(\phi) = V_{\min} + c_1\mathcal{D}^2\phi^2 + \frac{c_1\mathcal{D}^4}{3}\phi^4 + \cdots \tag{7}$$

which means that at an early enough epoch the "cosmic" fluid behaves like radiation [45] [$V(\phi) \propto \phi^4$], then evolves to the matter epoch [$V(\phi) \propto \phi^2$], and finishes with a phase that looks like a cosmological constant (see also [29]).

Changing now the variables from (a, ϕ) to (x_1, x_2) using the relations

$$x_1 = \sqrt{\tfrac{8}{3}}a^{3/2}\sinh(\mathcal{D}\phi) \qquad x_2 = \sqrt{\tfrac{8}{3}}a^{3/2}\cosh(\mathcal{D}\phi) \tag{8}$$

with $\mathcal{D}^2 = 3/8$ the Lagrangian (1) is written

$$L = \tfrac{1}{2}[(\dot{x}_1{}^2 + \tfrac{3}{4}c_2x_1^2) - (\dot{x}_2{}^2 + \tfrac{3}{4}(c_1 + c_2)x_2^2)] + \tfrac{1}{2}[3^{4/3}k(x_2^2 - x_1^2)^{1/3}]. \tag{9}$$

The scale factor ($a > 0$) in the UDM scenario is now given by

$$a = \left[\frac{3(x_2^2 - x_1^2)}{8}\right]^{1/3}, \tag{10}$$

which means that the new variables have to satisfy the following inequality: $x_2 \geq |x_1|$.

It is straightforward now from the Lagrangian (9) to write the corresponding Hamiltonian:

$$\mathcal{H} = \tfrac{1}{2}[(p_{x_1}^2 - \omega_1^2 x_1^2) - (p_{x_2}^2 - \omega_2^2 x_2^2)] - \tfrac{1}{2}[3^{4/3} k (x_2^2 - x_1^2)^{1/3}], \quad (11)$$

where $p_{x_1} = \dot{x}_1$, $p_{x_2} = -\dot{x}_2$ denote the canonical momenta, and $\omega_1^2 = \frac{3}{4}c_2$, $\omega_2^2 = \frac{3}{4}(c_1 + c_2)$ are the oscillators' "frequencies" with units of inverse of time and

$$\frac{\omega_2^2}{\omega_1^2} = 1 + \frac{c_2}{c_1} = \kappa \qquad (\kappa = 2). \quad (12)$$

The dynamics of the closed FLRW scalar field cosmologies has been investigated thoroughly in [43]. In particular, for a semiflat geometry ($k \to 0$) we have revealed cases where the dynamics of the system (see Sec. 3.1 in [43], orbit 5 in Fig. 1 scale factor vs time, and Fig. 4) is close to the concordance Λ cosmology, despite the fact that for the semiflat UDM model there is a strong indication of a chaotic behavior. In this paper we would like to investigate the potential of a spatially flat UDM scenario ($k = 0$) since the analysis of the CMB anisotropies have strongly suggested that the spatial geometry of the universe is flat [3]. Technically speaking, in the new coordinate system our dynamical problem is described well by two independent hyperbolic oscillators and thus the system is fully integrable. Indeed in the new coordinate system the corresponding equations of motion can be written as

$$\dot{p}_{x_1} = -\frac{\partial \mathcal{H}}{\partial x_1} = \omega_1^2 x_1, \qquad \dot{p}_{x_2} = -\frac{\partial \mathcal{H}}{\partial x_2} = -\omega_2^2 x_2$$

and it is routine to perform the integration to find the analytical solutions:

$$x_1(t) = A_1 \sinh(\omega_1 t + \theta_1) \qquad x_2(t) = A_2 \sinh(\omega_2 t + \theta_2), \quad (13)$$

where A_1, A_2, θ_1, and θ_2 are the integration constants of the problem. With the aid of Eq. (13) and assuming that the total energy ($\mathcal{H}$) of the system is zero, the above constants satisfy the following restriction:

$$A_1^2\omega_1^2 - A_2^2\omega_2^2 = 0 \Rightarrow \frac{A_1^2}{A_2^2} = \frac{\omega_2^2}{\omega_1^2} = \kappa. \quad (14)$$

As expected, the phase space of the current dynamical problem is simply described by two hyperbolas $p_{x_i}^2 - \omega_i^2 x_i^2 = \omega_i^2 A_i^2$ whose axes have a ratio $1/\omega_i$ ($i = 1, 2$).

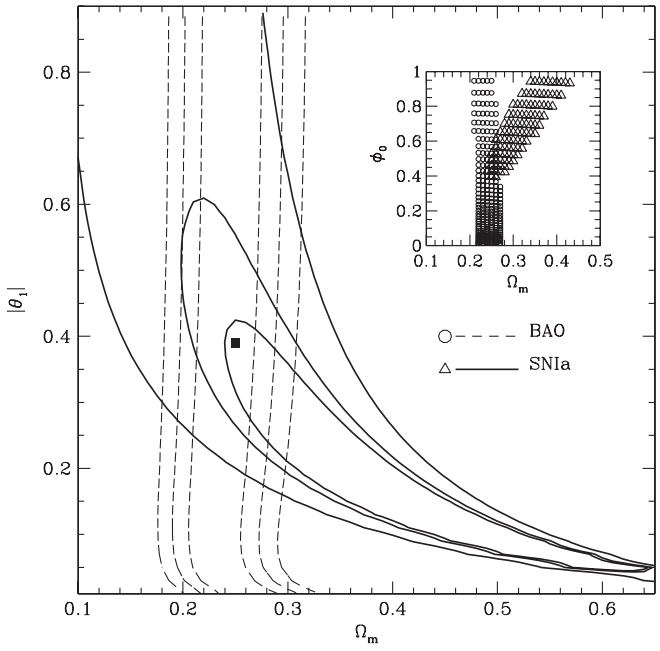

FIG. 1. Likelihood contours in the $(\Omega_m, |\theta_1|)$ plane. The contours correspond to 1σ, 2σ, and 3σ confidence levels. The thick (thin) contours correspond to the SNIa (BAOs) likelihoods while the solid square is the best-fit solution: $\Omega_m \simeq 0.25$ and $\theta_1 \simeq -0.39$. Inset panel: The solutions within 1σ contours in the (Ω_m, ϕ_0) plane, where ϕ_0 is the present value of the scalar field in geometrical units ($8\pi G = c \equiv 1$). Note that for Planck units ($G = c \equiv 1$) we have to multiply the ϕ_0 axis with $(8\pi)^{-1/2}$. Using the best-fit solution we find $\phi_0 \simeq 0.42$ or 0.084 in Planck units.

III. THE EVOLUTION OF THE UDM COSMOLOGICAL FUNCTIONS

In this section, with the aid of the basic hyperbolic functions, we analytically derive the predicted time dependence of the main cosmological functions in the UDM cosmological model.

A. Scalar field—potential versus time

If we combine Eq. (13) together with the initial parametrization [see Eq. (8)], we immediately obtain the following expressions:

$$\frac{x_1}{x_2} = \tanh(\mathcal{D}\phi) = \frac{\sqrt{\kappa}\sinh(\omega_1 t + \theta_1)}{\sinh(\omega_2 t + \theta_2)} = \Psi(t) \quad (15)$$

and after some algebra the evolution of the scalar field becomes

$$\phi(t) = \frac{1}{2\mathcal{D}} \ln\left[\frac{1 + \Psi(t)}{1 - \Psi(t)}\right]. \quad (16)$$

Using Eqs. (5) and (16) one can prove that

$$V(t) = \frac{4\omega_1^2}{3}\left[\frac{\kappa - \Psi^2(t)}{1 - \Psi^2(t)}\right]. \quad (17)$$

Now the range of Ψ values for which the UDM scalar field is well defined [due to Eq. (16)] is $\Psi \in (-1, 1)$. Evidently, when the system reaches the critical point $\phi = 0$ then $\Psi(t_m) = 0$ (or $V_{\min} = 4\omega_1^2\kappa/3$). For this to be the case we must have $t_m = -\theta_1/\omega_1$ and therefore $\theta_1 < 0$.

B. Scale factor—Hubble flow versus time

Inserting Eq. (13) into Eq. (10) the scale factor, normalized to unity at the present epoch, evolves in time as

$$a(t) \equiv \frac{a}{a_0} = \left[\frac{\sinh^2(\omega_2 t + \theta_2) - \kappa\sinh^2(\omega_1 t + \theta_1)}{\sinh^2(\omega_2 t_0 + \theta_2) - \kappa\sinh^2(\omega_1 t_0 + \theta_1)}\right]^{1/3}, \tag{18}$$

where t_0 is the present age of the universe in billion years. The constant θ_1 is related to θ_2 because at the singularity ($t = 0$), the scale factor has to be exactly zero [see Eq. (18)]. After some algebra, we find that

$$\theta_2 = \ln(-\sqrt{\kappa}\sinh\theta_1 + \sqrt{\kappa\sinh^2\theta_1 + 1}) \geq 0. \tag{19}$$

Furthermore, we investigate the circumstances under which an inflection point exists and therefore have an acceleration phase of the scale factor. This crucial period in the cosmic history corresponds to $\ddot{a}(t_I) = 0$ which implies that the condition

$$V(\phi_I) - \dot{\phi}_I{}^2 = 0$$

should contain roots which are real and such that $a \in (0, 1)$. The above equation is solvable because for $c_1, c_2 > 0$ the potential energy $[V(\phi)]$ takes only positive values. Knowing the integration constants $(\omega_1, \theta_1, \omega_2, \theta_2)$ of the current dynamical problem, we can calculate the inflection point by solving numerically the following equation:

$$2\dot{\Psi}^2(t_I) - \omega_1^2[\kappa - \Psi^2(t_I)][1 - \Psi^2(t_I)] = 0 \tag{20}$$

with

$$\dot{\Psi}(t) = \frac{\sqrt{\kappa}\omega_1\sum_{i=1}^{2}\nu_i\sinh(\omega_{3-i}t + \theta_{3-i})\cosh(\omega_i t + \theta_i)}{\sinh^2(\omega_2 t + \theta_2)}, \tag{21}$$

where $\nu_1 = 1$ and $\nu_2 = -\sqrt{\kappa}$.

In addition, the Hubble function predicted by the UDM model can be viewed as the sum of basic hyperbolic functions:

$$H(t) \equiv \frac{\dot{a}}{a} = \frac{2(x_2\dot{x}_2 - x_1\dot{x}_1)}{3(x_2^2 - x_1^2)} = \frac{2}{3}\omega_2 f(t) = H_0\frac{f(t)}{f(t_0)} \tag{22}$$

with

$$f(t) = \frac{\sum_{i=1}^{2}\nu_i\sinh(\omega_{3-i}t + \theta_{3-i})\cosh(\omega_{3-i}t + \theta_{3-i})}{\sinh^2(\omega_2 t + \theta_2) - \kappa\sinh^2(\omega_1 t + \theta_1)}, \tag{23}$$

where H_0 is the Hubble constant. In this work we use $H_0 = 100h\ \mathrm{K\,ms^{-1}\,Mpc^{-1}}$ with $h = 0.72$ [46] or $H_0 = h/9.778 \simeq 0.0736\ \mathrm{Gyr}^{-1}$ corresponding to $t_0 \approx H_0^{-1} \simeq 13.6$ Gyr. Also we can relate the frequency ω_2 of the hyperbolic oscillator in the x_2 axis with the well-known cosmological parameters. Indeed, ω_2 is given by

$$\omega_2 = \frac{3H_0\sqrt{1 - \Omega_m}}{2}, \tag{24}$$

while $\theta_1 \propto H_0 t_0$ has no units. Notice that Ω_m is the matter density at the present time.

IV. COSMOLOGICAL CONSTRAINTS AND PREDICTIONS

In this work we use the so-called baryonic acoustic oscillations (BAOs) in order to constrain the current cosmological models. BAOs are produced by pressure (acoustic) waves in the photon-baryon plasma in the early universe, generated by dark matter overdensities. First evidence of this excess was recently found in the clustering properties of the luminous Sloan Digital Sky Survey (SDSS) red galaxies [33,34] and it can provide a "standard ruler" with which we can put constraints on the cosmological models. For a spatially flat FLRW we use the following estimator:

$$A(\mathbf{p}) = \frac{\sqrt{\Omega_m}}{[z_s^2 H(a_s)/H_0]^{1/3}}\left[\int_{a_s}^{1}\frac{dy}{y^2 H(y)/H_0}\right]^{2/3} \tag{25}$$

measured from the SDSS data to be $A = 0.469 \pm 0.017$, where $z_s = 0.35$ [or $a_s = (1 + z_s)^{-1} \simeq 0.75$]. Therefore, the corresponding χ^2_{BAO} function is simply written

$$\chi^2_{\mathrm{BAO}}(\mathbf{p}) = \frac{[A(\mathbf{p}) - 0.469]^2}{0.017^2}, \tag{26}$$

where $\mathbf{p}$ is a vector containing the cosmological parameters that we want to fit.

Also, we additionally utilize the sample of 192 supernovae of Davies *et al.* [2]. In this case, the χ^2_{SNIa} function becomes

$$\chi^2_{\mathrm{SNIa}}(\mathbf{p}) = \sum_{i=1}^{192}\left[\frac{\mu^{\mathrm{th}}(a_i, \mathbf{p}) - \mu^{\mathrm{obs}}(a_i)}{\sigma_i}\right]^2, \tag{27}$$

where $a_i = (1 + z_i)^{-1}$ is the observed scale factor of the Universe, z_i is the observed redshift, μ is the distance modulus $\mu = m - M = 5\log d_{\mathrm{L}} + 25$, and $d_{\mathrm{L}}(a, \mathbf{p})$ is the luminosity distance

$$d_{\mathrm{L}}(a, \mathbf{p}) = \frac{c}{a}\int_a^1\frac{dy}{y^2 H(y)}, \tag{28}$$

where c is the speed of light ($\equiv 1$ here). Finally we can combine the above probes by using a joint likelihood analysis:

$$\mathcal{L}_{\mathrm{tot}}(\mathbf{p}) = \mathcal{L}_{\mathrm{BAO}} \times \mathcal{L}_{\mathrm{SNIa}} \qquad \chi^2_{\mathrm{tot}}(\mathbf{p}) = \chi^2_{\mathrm{BAO}} + \chi^2_{\mathrm{SNIa}},$$

in order to put even further constraints on the parameter space used. Note that we define the likelihood estimator [47] as $\mathcal{L}_j \propto \exp[-\chi_j^2/2]$.

A. The standard Λ cosmology

Without wanting to appear too pedagogical, we remind the reader of some basic elements of the concordance Λ cosmology. In this framework, the normalized scale factor of the universe is

$$a^{\Lambda}(t) = \left(\frac{\Omega_m}{1-\Omega_m}\right)^{1/3} \sinh^{2/3}\omega_2 t. \quad (29)$$

The Hubble function is written as

$$H(t) = \tfrac{2}{3}\omega_2 f(t) = \tfrac{2}{3}\omega_2 \coth\omega_2 t. \quad (30)$$

Comparing the Λ model with the observational data (we sample $\Omega_m \in [0.1, 1]$ in steps of 0.01), we find that the best-fit value is $\Omega_m = 0.26 \pm 0.01$ with $\chi^2_{\rm tot}(\Omega_m) \simeq 195$ (dof = 192) in a very good agreement with the 5 years WMAP data [4]. The inflection point takes place at

$$t_I^{\Lambda} = \frac{1}{\omega_2}\sinh^{-1}\left(\frac{1}{2}\right) \qquad a_I^{\Lambda} = \left[\frac{\Omega_m}{2(1-\Omega_m)}\right]^{1/3}. \quad (31)$$

Therefore, we estimate $\omega_2 \simeq 1.29 H_0 \simeq 0.095$ Gyr^{-1}, $t_I^{\Lambda} \simeq 0.51 t_0$, and $a_I^{\Lambda} \simeq 0.56$. The deceleration parameter at the present time is $q_0 \equiv -\ddot{a}/\dot{a}^2|_{a=1} \simeq -0.61$.

B. The parametric dark energy model

In this case we use a simple parametrization for the dark energy equation of state parameter which is based on a Taylor expansion around the present time (see Chevallier and Polarski [48] and Linder [49], hereafter CPL)

$$w(a) = w_0 + w_1(1-a). \quad (32)$$

The Hubble parameter is given by

$$H(a) = H_0[\Omega_m a^{-3} + (1-\Omega_m)a^{-3(1+w_0+w_1)}e^{3w_1(a-1)}]^{1/2}, \quad (33)$$

where w_0 and w_1 are constants. We sample the unknown parameters as follows: $w_0 \in [-2, -0.4]$ and $w_1 \in [-2.6, 2.6]$ in steps of 0.01. We find that for $\Omega_m = 0.26$ the overall likelihood function peaks at $w_0 = -1.20^{+0.28}_{-0.20}$ and $w_1 = 1.14^{+1.0}_{-1.9}$ while the corresponding $\chi^2_{\rm tot}(w_0, w_1)$ is 193.6 (dof = 191). The deceleration parameter at the present time is $q_0 \simeq -0.83$.

C. The variable Chaplygin gas as an alternative to dark energy

Let us consider now a completely different model, namely, the variable Chaplygin gas (hereafter VCG) which corresponds to a Born-Infeld tachyon action [50,51]. Recently, an interesting family of Chaplygin gas models was found to be consistent with the current observational data [52]. In the framework of a spatially flat FLRW metric, it can be shown that the Hubble function takes the following formula:

$$H(a) = H_0[\Omega_b a^{-3} + (1-\Omega_b) \times \sqrt{B_s a^{-6} + (1-B_s)a^{-n}}]^{1/2}, \quad (34)$$

where $\Omega_b \simeq 0.021 h^{-2}$ is the density parameter for the baryonic matter [53] and $B_s \in [0.01, 0.51]$ in steps of 0.01 and $n \in [-4, 4]$ in steps of 0.02. The corresponding effective equation of state parameter $w(a) = P_{\rm DE}/\rho_{\rm DE}$ is related to $H(a)$ according to

$$w(a) = \frac{-1 - \frac{2}{3}a\frac{d\ln H}{da}}{1 - (\frac{H_0}{H})^2\Omega_m a^{-3}}, \quad (35)$$

while the effective matter density parameter is $\Omega_m^{\rm eff} = \Omega_b + (1-\Omega_b)\sqrt{B_s}$. We find that the best-fit parameters are $B_s = 0.07 \pm 0.02$ and $n = 1.06 \pm 0.33$ ($\Omega_m^{\rm eff} \simeq 0.29$) with $\chi^2_{\rm tot}(B_s, n) = 193.7$ (dof = 191) and the present value of the deceleration parameter is $q_0 \simeq -0.60$.

D. The UDM comparison with other dark energy models

In order to predict analytically the time evolution of the main cosmological functions [$\phi(t)$, $a(t)$, $H(t)$, and $w(t)$], we have to define the corresponding unknown constants of the problem ($\omega_1, \theta_1, \omega_2, \theta_2$). At the same time, from the restrictions found in Sec. III [see Eqs. (12), (19), and (24)], we can reduce the parameter space to (Ω_m, θ_1). We do so by fitting the predictions of the UDM cosmological model and recent observational data. Here, we use $\Omega_m \in [0.1, 1]$ and $\theta_1 \in [-1, 0]$ in steps of 0.01.

Figure 1 (thin dashed lines) shows the 1σ, 2σ, and 3σ confidence levels in the ($\Omega_m, |\theta_1|$) plane when using BAOs. Obviously, the θ_1 parameter is not constrained by this analysis and all the values in the interval $-1 \leq \theta_1 \leq 0$ are acceptable. However, the BAOs statistical analysis puts constraints on the matter density parameter $\Omega_m \simeq 0.25$.

Therefore, in order to put further constraints on θ_1 we additionally utilize the SNIa data. In Fig. 1 (thick solid lines), we present the SNIa likelihood contours and we find that the best-fit solution is $\Omega_m \simeq 0.4$ and $\theta_1 \simeq -0.05$. The joint likelihood function peaks at $\Omega_m = 0.25^{+0.02}_{-0.01}$ and $\theta_1 = -0.39^{+0.04}_{-0.08}$ ($\theta_2 \simeq 0.54$) with $\chi^2_{\rm tot}(\Omega_m, |\theta_1|) \simeq 194.1$ (dof = 191). Note that the errors of the fitted parameters represent 1σ uncertainties. In the inset plot of Fig. 1 we provide the solutions (circles—BAOs and triangles—SNIa) within 1σ contours in the (Ω_m, ϕ_0) plane, where ϕ_0 is the present value of the scalar field. The corresponding best-fit value of the scalar field [see Eqs. (15) and (16)] is $\phi_0 \simeq 0.42$ or 0.084 in Planck units ($G = c \equiv 1$), while the frequencies are $\omega_1 \simeq 0.067$ Gyr^{-1} and $\omega_2 \simeq 0.095$ Gyr^{-1}. It is interesting to mention that, although the frequency ($\omega_1 \sim 0.9 H_0$) of the hyperbolic oscillator in the x_1 axis is somewhat less than the present expansion rate of the universe, the ω_2 is equal to the value predicted by the Λ cosmology (see Sec. IV A).

Knowing now the parameter space $(\omega_1, \theta_1, \omega_2, \theta_2)$ we investigate, in more detail, the correspondence of the UDM model with the different dark energy models (see Secs. IV A, IV B, and IV C) in order to show the extent to which they compare. Our analysis provides an evolution of the UDM scale factor seen in the upper panel of Fig. 2 as the solid line, which closely resembles, especially at late times ($0.6 < a \leq 1.5$), the corresponding scale factor of the Λ (short dashed), VCG (dot dashed), and CPL (long dashed). Note that the UDM deceleration parameter at the present time is $q_0 \simeq -0.62$. However, for $a > 1.5$, the CPL and the VCG scale factors evolve more rapidly than the other two models (UDM and Λ cosmology). Also it is clear that an inflection point [$\ddot{a}(t_I) = 0$] is present in the evolution of the UDM scale factor. The UDM inflection point is located at $t_I \simeq 0.46 t_0$ which corresponds to $a_I \simeq 0.61$ and

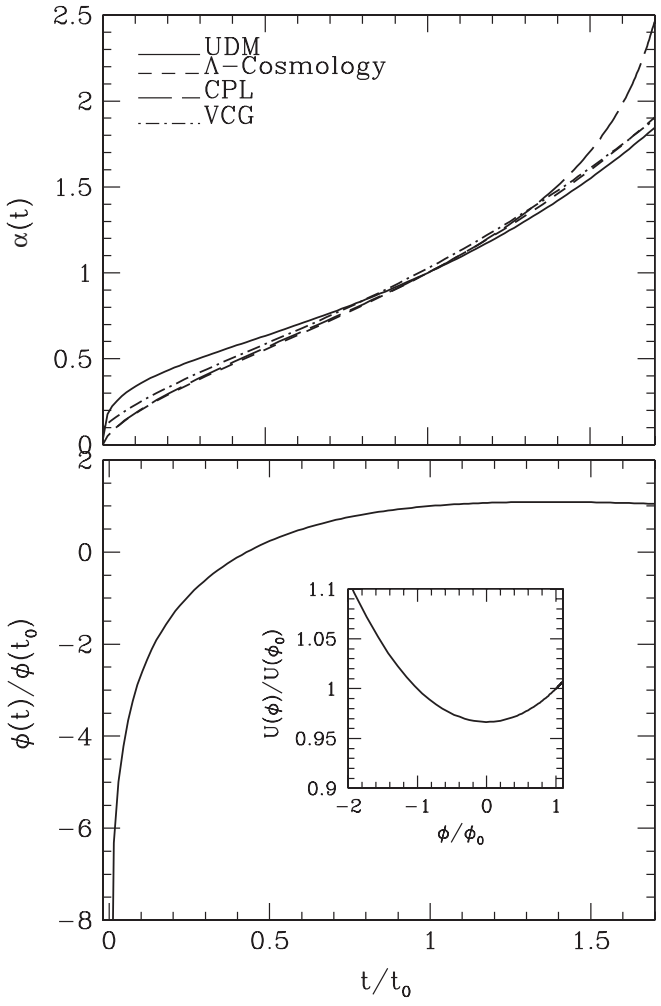

FIG. 2. Upper panel: Comparison of the scale factor provided by the UDM model (solid line) with the traditional Λ cosmology (short dashed line), VCG (dot dashed), and CPL (long dashed) dark energy models. Bottom panel: The evolution of the scalar field. In the inset panel we present the behavior of the potential normalized to unity at the present time. Note that $t_0 \approx H_0^{-1} \simeq 13.6$ Gyr is the present age of the universe.

is somewhat different than the value predicted from the usual Λ cosmology (see Sec. IV A). Before the inflection point, the UDM appears to be more decelerated from the other three dark energy cosmological models due to the fact that the second term [$\propto \sinh^2(\omega_1 t + \theta_1)$] in Eq. (18) plays an important role. From Fig. 2 it becomes clear that the UDM model reaches a maximum deviation from the other three dark energy models prior to $a \sim 0.15$ ($z \sim 5.5$). In order to investigate whether the expansion of the observed universe follows such a possibility, we need a visible distance indicator (better observations) at redshifts $z > 2$.

The evolution of the scalar field is presented in the bottom panel of Fig. 2, while in the inset figure we plot the scalar field dependence of the potential energy normalized to unity at the present time. As we have stated in Sec. III A there is one minimum at $\phi = 0$ that corresponds to $t_m = -\theta_1/\omega_1 \sim 0.4 t_0$. To conclude, we plot in Fig. 3 the relative deviations of the distance modulus, $\Delta(m - M)$, of the dark energy models used here from the traditional Λ cosmology. Notice that the open points represent the following deviation: $(m - M)_{\rm SNIa} - (m - M)_{\Lambda}$. Within the SNIa redshift range $0.016 \leq z \leq 1.775$ ($0.360 \leq a \leq 0.984$), the VCG distance modulus is close to the Λ one. The largest deviations of the distance moduli occur at redshifts around 0.5–1 for the UDM and 1.1–1.5 for the CPL model, respectively.

E. The equation of state parameter

We would like to end this section with a discussion on the dark energy equation of state. As we have stated already in the introduction, there is a possibility for the equation of state parameter to be a function of time rather

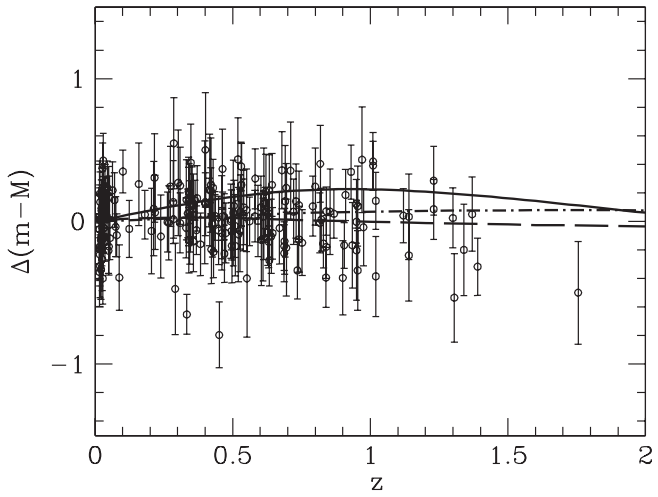

FIG. 3. Residual magnitudes (relative to the traditional $\Omega_\Lambda = 0.74$, $\Omega_m = 0.26$ model) of 192 SNIa data (open points) from [2] as a function of redshift. For comparison we plot the $\Delta(m - M)_{\rm UDM\text{-}\Lambda}$ (solid line), $\Delta(m - M)_{\rm CPL\text{-}\Lambda}$ (long dashed line), and $\Delta(m - M)_{\rm VCG\text{-}\Lambda}$ (dot dashed line).

than a constant ratio between the pressure and the energy density. Within the framework of the scalar field cosmology, the equation of state parameter is derived from the field model and in general it is a complicated function of time, even when the potential is written as a simple function of the scalar field. In our case we have

$$w(t) = \frac{P_\phi}{\rho_\phi} = \frac{\dot\phi^2 - 2V(\phi)}{\dot\phi^2 + 2V(\phi)} \tag{36}$$

or else [see Eqs. (16) and (17)]

$$w(t) = \frac{\dot\Psi^2(t) - \omega_1^2[\kappa - \Psi^2(t)][1 - \Psi^2(t)]}{\dot\Psi^2(t) + \omega_1^2[\kappa - \Psi^2(t)][1 - \Psi^2(t)]}. \tag{37}$$

Note that Λ models can be described by scalar models with w strictly equal to -1. Using our best-fit parameters we present in the left panel of Fig. 4 the equation of state parameter as a function of the scale factor for the different dark energy models. The UDM model (solid line) is the only case that provides positive values for the equation of state parameter at early epochs. We have checked the UDM scenario against the cosmic coincidence problem (why the matter energy density and the dark energy density are of the same order at the present epoch) by utilizing the basic tests proposed by [42]. These are: (a) at early enough times the equation of state parameter tends to its maximum value, $w \to +1$, which means that the dark energy density initially takes large values. So as long as the scalar field rolls down the potential energy $V(\phi)$ decreases rapidly and the kinetic energy $T_\phi = \dot\phi^2/2$ takes a large value, (b) then ϕ continues to roll down, the dark energy density decreases and the equation of state parameter remains close to unity for a quite long period of time ($a < 0.2$), and (c) for $0.2 \le a \le 0.95$ the equation of state parameter is a decreasing function of time and it becomes negative at $a > 0.56$. Before that epoch, the potential energy of the scalar field remains less than the kinetic energy (see the inset plot in the left panel of Fig. 4) and the equation of state parameter (or the scalar field) resembles background matter. In a special case where $w = 0$ [or $T_\phi \simeq V(\phi)$], the equation of state behaves exactly like that of pressureless matter. For $w = -1/3$ we reach the same expansion as in an open universe, because the dark energy density evolves as a^{-2} and has no effect on $\ddot a$. In fact, we verify that prior to the inflection point $w(t_I) \simeq -0.334$, which means that after t_I the accelerating expansion of the Universe starts. Finally, $w \simeq -1$ close to the present epoch $a \sim 1$ and the scalar field is effectively frozen (the same situation seems to hold also in the limit $a \gg 1$). This is to be expected because at this period the scalar field varies slowly with time (see the inset panel of Fig. 4), so that $T_\phi \ll V(\phi)$ and the dark energy fluid asymptotically reaches the de-Sitter regime (cosmological constant).

In order to conclude this discussion, it is interesting to point out that we also investigate the sensitivity of the above results to the matter density parameter. As an example, in the right panel of Fig. 4 we present the evolution of the equation of state parameter for $(\Omega_m, \theta_1) = (0.73, -1)$ [upper line] and $(\Omega_m, \theta_1) = (0.19, -0.1)$ [bottom line]. We confirm that in the range $\Omega_m \in (0.19, 0.73)$ and $\theta_1 \in (-1, -0.1)$ the general behavior (described before) of the functional form of the equation of state pa-

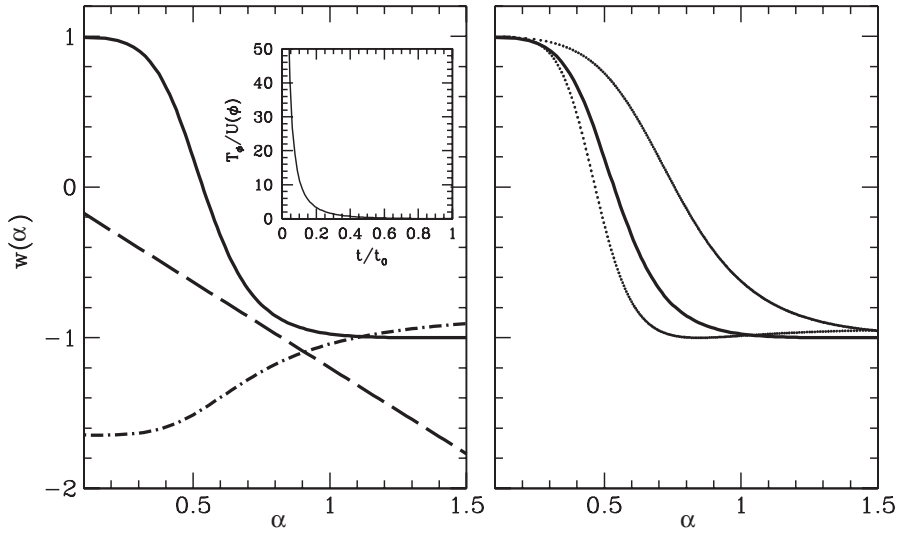

FIG. 4. Left panel: The equation of state parameter as a function of the scale factor of the Universe. The lines correspond to UDM (solid), CPL (long dashed), and VCG (dot dashed). In the inset panel we present the time evolution of $T_\phi/V(\phi)$. Note that T_ϕ is the kinetic energy of the scalar and $V(\phi)$ is the potential. Right panel: The functional form of the equation of state parameter for various UDM models. The upper line corresponds to $(\Omega_m, \theta_1) = (0.73, -1)$ while the bottom line corresponds to $(\Omega_m, \theta_1) = (0.19, -0.1)$. Note that the solid thick line corresponds to the best-fit parameters $(\Omega_m, \theta_1) = (0.25, -0.39)$. We find that initially all the UDM models [$\Omega_m \in (0.19, 0.73)$, $\theta_1 \in (-1, -0.1)$] start from $w \to +1$ and they reach $w \simeq O(-1)$ close to the present time.

rameter is an intermediate case between the above lines for $a \leq 1$ and thus it depends weakly on the values of the parameter space (Ω_m, θ_1). Therefore, our main cosmological results for the UDM scenario persist for all physical values of Ω_m and it strongly indicates that the UDM model overpasses the cosmic coincidence problem.

V. EVOLUTION OF MATTER PERTURBATIONS

In this section we attempt to study the dynamics at small scales by generalizing the basic linear and nonlinear equations which govern the behavior of the matter perturbations within the framework of a UDM flat cosmology. Also we compare our predictions with those found for the dark energy models used in this work (see Secs. IV A, IV B, and IV C). This can help us to understand better the theoretical expectations of the UDM model as well as the variants from the other dark energy models.

A. The Evolution of the linear growth factor

The evolution equation of the growth factor for models where the dark energy fluid has a vanishing anisotropic stress and the matter fluid is not coupled to other matter species is given by [54–56]

$$\frac{\mathrm{d}^2 D}{\mathrm{d}N^2} + \left(2 + \frac{1}{H}\frac{\mathrm{d}H}{\mathrm{d}N}\right)\frac{\mathrm{d}D}{\mathrm{d}N} - \frac{3}{2}\Omega_m(a)D = 0, \qquad (38)$$

where $N = \ln a$ and $\Omega_m(a) = \Omega_m a^{-3} H_0^2/H^2(a)$. Useful expressions of the growth factor can be found for the ΛCDM cosmology in [54], for the quintessence scenario ($w = $ const) in [57–60], for dark energy models with a time varying equation of state in [61], and for the scalar tensor models in [62]. In the upper panel of Fig. 5 we present the growth factor evolution which is derived by solving numerically Eq. (38), for the four dark energy models (including the UDM). Note that the growth factors are normalized to unity at the present time. The behavior of the UDM growth factor (solid line) has the expected form, i.e. it is an increasing function of the scale factor. Also we find that the growth factor in the UDM model is almost an intermediate case between the VCG (dot dashed line) and CPL (long dashed line) models, respectively. In the bottom panel of Fig. 5 we show the deviation, $(1 - D_{\mathrm{DE}}/D_\Lambda)\%$, of the growth factors $D_{\mathrm{DE}}(a)$ for the current dark energy models with respect to the Λ solution $D_\Lambda(a)$. Assuming now that clusters have formed prior to the epoch of $z_f \simeq 1.4$ ($a_f \sim 0.42$), in which the most distant cluster has been found [63], the UDM scenario (open triangles) deviates from the Λ solution by 4.2% while the CPL (open circles) and VCG (solid squares) deviate by -1.5% and 5.1%, respectively. Also at the Λ-inflection point ($a_I^\Lambda \simeq 0.56$), we find the following results: (i) UDM-Λ 3.3%, (ii) CPL-Λ -0.4%, and (iii) VCG-Λ 3.2%. To conclude this discussion it is obvious that for $a \geq 0.7$ the UDM growth factor

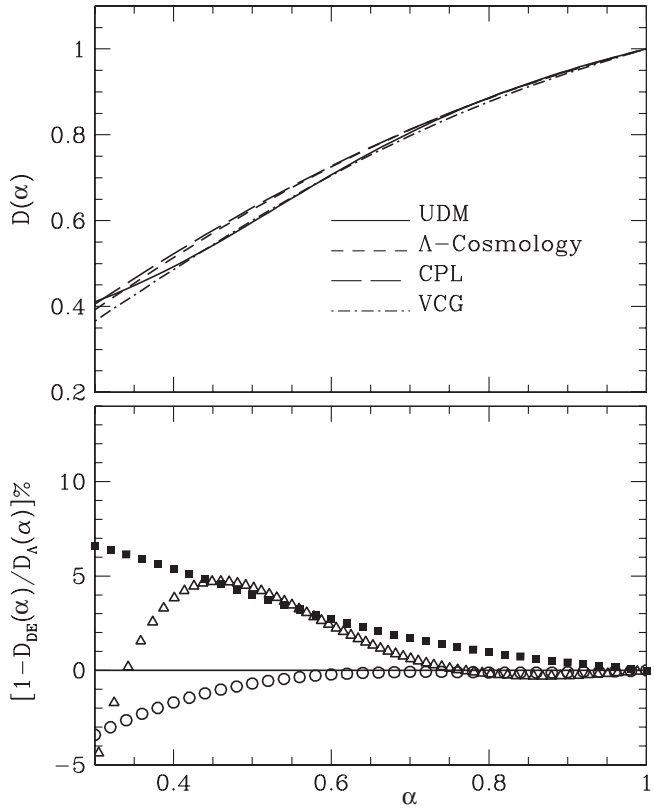

FIG. 5. Upper panel: The evolution of the growth factor for different dark energy models. The lines correspond to UDM (solid), VCG (dot dashed), Λ (short dashed), and CPL (long dashed) models. Bottom panel: The deviation $(1 - D_{\mathrm{DE}}/D_\Lambda)\%$ of the growth factor for various dark energy models with respect to the Λ solution. The points represent the comparison: (a) UDM-Λ (open triangles), (b) VCG-Λ (solid squares), and (c) CPL-Λ (open circles).

tends to the Λ solution (the same situation holds for the CPL model but with $a \geq 0.55$).

B. The spherical collapse model

The so-called spherical collapse model, which has a long history in cosmology, is a simple but still a fundamental tool for understanding how a small spherical patch [with radius $R(t)$] of homogeneous overdensity forms a bound system via gravitation instability [64]. From now on, we will call a_t the scale factor of the universe where the overdensity reaches its maximum expansion ($\dot{R} = 0$) and a_f the scale factor in which the sphere virializes, while R_t and R_f the corresponding radii of the spherical overdensity. Note that in the spherical region, $\rho_{mc} \propto R^{-3}$ is the matter density while ρ_{ϕ_c} will denote the corresponding density of the dark energy. In order to address the issue of the dark energy in the gravitationally bound systems (clusters of galaxies), we can consider the following assumptions: (i) clustered dark energy considering that the whole system virializes (matter and dark energy), (ii) the dark energy

remains clustered but now only the matter virializes, and (iii) the dark energy remains homogeneous and only the matter virializes (for more details see [65–68]). Note, that in this work we are using the third possibility.

Here we review only some basic concepts of the problem based on the assumption that the dark energy component under a scale of galaxy clusters can be treated as being homogeneous: $\rho_{\phi_c}(t) = \rho_{\phi}(t)$, $\phi_c(t) = \phi(t)$, and $w_c(t) = w(t)$. In general the evolution of the spherical perturbations as the latter decouple from the background expansion is given by the Raychaudhuri equation:

$$3\ddot{R} = -4\pi GR[\rho_{mc} + \rho_{\phi_c}(1 + w_c)] \quad \text{here } 4\pi G \equiv 1/2. \tag{39}$$

Now within the cluster region the evolution of the dark energy component is written as (see [65])

$$\dot{\rho}_{\phi_c} + 3\frac{\dot{R}}{R}(1 + w_{\phi_c})\rho_{\phi_c} = \Gamma \tag{40}$$

while if we consider a scalar field the above equation becomes

$$\ddot{\phi}_c + 3\frac{\dot{R}}{R}\dot{\phi}_c + U'(\phi_c) = \frac{\Gamma}{\dot{\phi}}, \tag{41}$$

where

$$\Gamma = -3\left(\frac{\dot{a}}{a} - \frac{\dot{R}}{R}\right)\dot{\phi}_c^2. \tag{42}$$

Figure 6 presents examples of $R(t)$ obtained for the UDM (solid line) and for the concordance Λ model (dashed line).

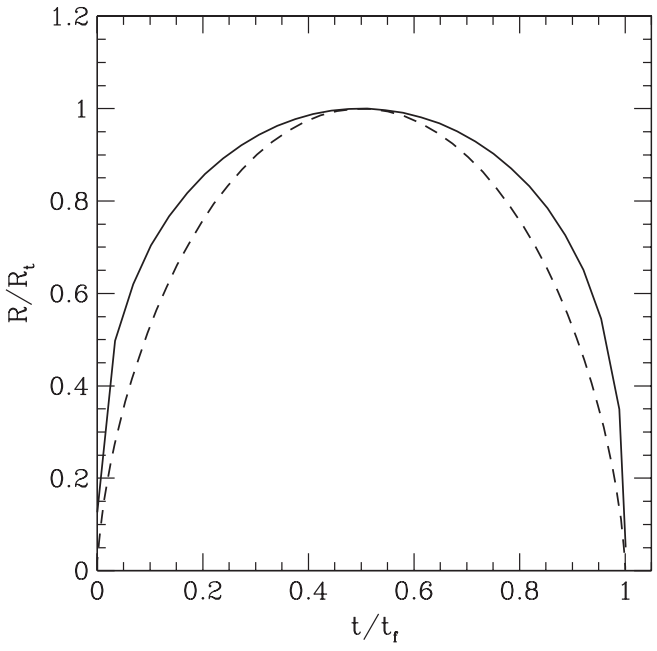

FIG. 6. Evolution of radius of a collapsing overdense region. The solid and the dashed line corresponds to the UDM ($\Omega_m = 0.25$) and Λ cosmology ($\Omega_m = 0.26$), respectively.

The time needed for a spherical shell to recollapse is twice the turn-around time, $t_f \simeq 2t_t$.

On the other hand, utilizing both the virial theorem and the energy conservation we reach to the following condition:

$$\left[\frac{1}{2}R\frac{\partial}{\partial R}(U_G + U_{\phi_c}) + U_G + U_{\phi_c}\right]^{a=a_f} = [U_G + U_{\phi_c}]^{a=a_t} \tag{43}$$

where $U_G = -3GM^2/5R$ is the potential energy and $U_{\phi_c} = -4\pi GM(1 + 3w_c)\rho_{\phi_c}R^2/5$ is the potential energy associated with the dark energy for the spherical overdensity (see [65,66]; in our case $4\pi G \equiv 1/2$). Using the above formulation, we can obtain a cubic equation that relates the ratio between the virial R_f and the turn-around outer radius R_t the so-called collapse factor ($\lambda = R_f/R_t$). Notice that Eq. (43) is valid when the ratio of the system's dark energy to the matter's densities at the time of the turn-around takes relatively small values [67]. Of course in the case of $w_c = -1$ the above expressions get the usual form for Λ cosmology [59,69] while for an Einstein–de-Sitter model ($\Omega_m = 1$) we have $\lambda = 1/2$. Finally solving numerically Eq. (43) [it can be done also analytically], we calculate the collapse factor. In particular, Fig. 7 shows the behavior of the collapse factor for the current cosmological models starting from the UDM (solid line), Λ (short dashed), VCG (dot dashed), and CPL (long dashed). We find that the collapse factor lies in the range $0.43 \leq \lambda \leq 0.50$ in agreement with previous studies [59,65–68,70,71]. Prior to the cluster formation epoch ($z_f \simeq 1.4$), the UDM scenario appears to produce more bound systems with respect to the other dark energy models. Indeed, we find the following values: $\lambda_{\rm UDM} \simeq 0.44$, $\lambda_{\Lambda} \simeq 0.49$, $\lambda_{\rm CPL} \simeq 0.48$, and $\lambda_{\rm VCG} \simeq 0.50$. Also it becomes clear that the UDM collapse factor decreases slowly with the redshift of virialization z_f, due to its positive equation of state parameter. This is also

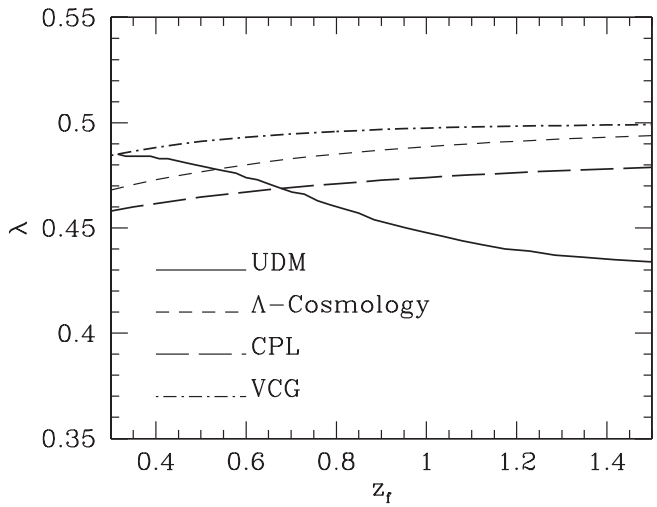

FIG. 7. The collapse factor versus the redshift of virialization for various dark energy models.

incorporated by the fact that at early epochs the cosmic expansion of the UDM model is much more decelerated than in the other three dark energy models. The latter result is in agreement with those obtained by [65]. They found a similar behavior for the collapse factor by considering several potentials with an exponential phase.

VI. CONCLUSIONS

In this work we investigate analytically and numerically the large and small scale dynamics of the scalar field FLRW flat cosmologies in the framework of the so-called *unified dark matter* scenario. In particular, using a Hamiltonian formulation we find that the time evolution of the basic cosmological functions is described in terms of hyperbolic functions. This theoretical approach yields analytical solutions which can accommodate a late time accelerated expansion, equivalent to either the dark energy or the standard Λ models. Furthermore, based on a joint likelihood analysis using the SNIa data and the baryonic acoustic oscillations, we put tight constraints on the main cosmological parameters of the UDM cosmological model. In particular, we find $\Omega_m \simeq 0.25$ and the scalar field at the present time is $\phi_0 \simeq 0.42$ or 0.084 (in Planck units). Also, we compare the UDM scenario with various dark energy models: namely, Λ cosmology, parametric dark energy model, and variable Chaplygin gas. We find that the cosmological behavior of the UDM scalar field model is in a good agreement, especially after the inflection point, with those predicted by the above dark energy models although there are some differences especially at early epochs. In particular, we reveal that the UDM scalar field cosmology has three important differences over the other three dark energy models considered:

(i) It can pick up positive values of the equation of state parameter at large redshifts ($z > 0.8$). Also, it behaves relatively well with respect to the cosmic coincidence problem.

(ii) At early enough epochs ($a \sim 0.15$ or $z \sim 5.5$), the cosmic expansion in the UDM model is much more decelerated than in the other three dark energy models. In order to investigate whether the expansion of the observed universe has the above property, we need a visible distance indicator (better observations) at high redshifts ($2 \leq z \leq 6$).

(iii) Close to the cluster formation epoch, its collapse factor $\lambda_{\rm UDM}$ is less than 12% of the corresponding factor of the other three dark energy models. This feature points to the direction that perhaps the λ parameter can be used as a cosmological tool.

ACKNOWLEDGMENTS

We thank Professor George Contopoulos, Dr. Manolis Plionis, and the anonymous referee for their useful comments and suggestions. G. Lukes-Gerakopoulos was supported by the Greek Foundation of State Scholarships (IKY).

[1] A. G. Riess *et al.*, Astrophys. J. **659**, 98 (2007).
[2] W. M. Wood-Vasey *et al.*, Astrophys. J. **666**, 694 (2007); T. M. Davis *et al.*, Astrophys. J. **666**, 716 (2007).
[3] D. N. Spergel *et al.*, Astrophys. J. Suppl. Ser. **170**, 377 (2007).
[4] E. Komatsu *et al.*, arXiv:0803.0547.
[5] B. Ratra and P. J. E. Peebles, Phys. Rev. D **37**, 3406 (1988).
[6] S. Weinberg, Rev. Mod. Phys. **61**, 1 (1989).
[7] C. Wetterich, Astron. Astrophys. **301**, 321 (1995).
[8] R. R. Caldwell, R. Dave, and P. J. Steinhardt, Phys. Rev. Lett. **80**, 1582 (1998).
[9] A. Kamenshchik, U. Moschella, and V. Pasquier, Phys. Lett. B **511**, 265 (2001).
[10] R. R. Caldwell and E. V. Linder, Phys. Rev. Lett. **95**, 141301 (2005).
[11] P. J. Peebles and B. Ratra, Rev. Mod. Phys. **75**, 559 (2003).
[12] P. Brax and J. Martin, Phys. Lett. B **468**, 40 (1999).
[13] A. Feinstein, Phys. Rev. D **66**, 063511 (2002).
[14] L. P. Chimento and A. Feinstein, Mod. Phys. Lett. A **19**, 761 (2004).
[15] A. W. Brookfield, C. van de Bruck, D. F. Mota, and D. Tocchini-Valentini, Phys. Rev. Lett. **96**, 061301 (2006).
[16] E. J. Copeland, M. Sami, and S. Tsujikawa, Int. J. Mod. Phys. D **15**, 1753 (2006).
[17] C. G. Boehmer and T. Harko, Eur. Phys. J. C **50**, 423 (2007).
[18] J. A. Frieman, M. S. Turner, and D. Huterer, Annu. Rev. Astron. Astrophys. **46**, 385 (2008).
[19] M. Ozer and O. Taha, Nucl. Phys. **B287**, 776 (1987).
[20] P. J. Peebles and B. Ratra, Astrophys. J. **325**, L17 (1988).
[21] M. S. Turner and M. White, Phys. Rev. D **56**, R4439 (1997).
[22] T. Padmanabhan, Phys. Rep. **380**, 235 (2003).
[23] A. D. Dolgov, M. V. Sazhin, and Y. B. Zeldovich, *Basics of Moderm Cosmology* (Frontieres, Gif sur Yvette, France, 1990).
[24] V. Sahni and L. Wang, Phys. Rev. D **62**, 103517 (2000).
[25] D. I. Santiago and A. S. Silbergleit, Phys. Lett. A **268**, 69 (2000).
[26] A. A. Sen and S. Sethi, Phys. Lett. B **532**, 159 (2002).
[27] A. Kehagias and G. Kofinas, Classical Quantum Gravity **21**, 3871 (2004).
[28] V. Gorini, A. Kamenshchik, U. Moschella, V. Pasquier, and A. Starobinsky, Phys. Rev. D **72**, 103518 (2005).

[29] D. Bertacca, S. Matarrese, and M. Pietroni, Mod. Phys. Lett. A **22**, 2893 (2007).
[30] A. Y. Kamenshchik, U. Moschella, and V. Pasquier, Phys. Lett. B **511**, 265 (2001).
[31] N. Bilic, G. B. Tupper, and R. D. Viollier, Phys. Lett. B **535**, 17 (2002).
[32] F. Takahashi and T. T. Yanagida, Phys. Lett. B **635**, 57 (2006).
[33] D. J. Eisenstein *et al.*, Astrophys. J. **633**, 560 (2005).
[34] N. Padmanabhan *et al.*, Mon. Not. R. Astron. Soc. **378**, 852 (2007).
[35] D. N. Page, Classical Quantum Gravity **1**, 417 (1984).
[36] Note that in this work we set $8\pi G = c \equiv 1$ which corresponds to $\mathcal{D}^2 = 3/8$. For Planck units we have to set $G = c \equiv 1$ with $\mathcal{D}^2 = 3\pi$. For SI units we have $\mathcal{D}^2 = 3\pi G/c^2$.
[37] C. Wetterich, Nucl. Phys. **B302**, 668 (1988).
[38] I. Zlatev, L. M. Wang, and P. J. Steinhardt, Phys. Rev. Lett. **82**, 896 (1999).
[39] A. V. Toporensky, SIGMA **2**, 37 (2006).
[40] M. S. Turner, Phys. Rev. D **28**, 1243 (1983).
[41] F. Lucchin and S. Matarrese, Phys. Rev. D **32**, 1316 (1985).
[42] P. J. Steinhardt, L. Wang, and I. Zlatev, Phys. Rev. D **59**, 123504 (1999).
[43] G. Lukes-Gerakopoulos, S. Basilakos, and G. Contopoulos, Phys. Rev. D **77**, 043521 (2008).
[44] V. Gorini, A. Kamenshchik, U. Moschella, and V. Pasquier, Phys. Rev. D **69**, 123512 (2004).
[45] R. J. Scherrer, Phys. Rev. Lett. **93**, 011301 (2004).
[46] W. L. Freedman, Astrophys. J. **553**, 47 (2001).
[47] Likelihoods are normalized to their maximum values.
[48] M. Chevallier and D. Polarski, Int. J. Mod. Phys. D **10**, 213 (2001).
[49] E. V. Linder, Phys. Rev. Lett. **90**, 091301 (2003).
[50] M. C. Bento, O. Bertolami, and A. A. Sen, Phys. Rev. D **70**, 083519 (2004).
[51] Z. K. Guo and Y. Z. Zhang, Phys. Lett. B **645**, 326 (2007); arXiv:astro-ph/050979.
[52] M. Makler, S. Q. de Oliveira, and I. Waga, Phys. Lett. B **555**, 1 (2003); M. C. Bento, O. Bertolami, and A. A. Sen, Phys. Lett. B **575**, 172 (2003); A. Dev, J. S. Alcaniz, and D. Jain, Phys. Rev. D **67**, 023515 (2003); Y. Gong and C. K. Duan, Mon. Not. R. Astron. Soc. **352**, 847 (2004); Z. H. Zhu, Astron. Astrophys. **423**, 421 (2004); L. Amendola, I. Waga, and F. Finelli, J. Cosmol. Astropart. Phys. 11 (2005) 009.
[53] D. Kirkman, D. Tytler, N. Suzuki, J. M. O'Meara, and D. Lubin, Astrophys. J. Suppl. Ser. **149**, 1 (2003).
[54] P. J. E. Peebles, *Principles of Physical Cosmology* (Princeton University Press, Princeton, New Jersey, 1993).
[55] H. F. Stabenau and B. Jain, Phys. Rev. D **74**, 084007 (2006).
[56] P. J. Uzan, Gen. Relativ. Gravit. **39**, 307 (2007).
[57] V. Silveira and I. Waga, Phys. Rev. D **50**, 4890 (1994).
[58] L. Wang and J. P. Steinhardt, Astrophys. J. **508**, 483 (1998).
[59] S. Basilakos, Astrophys. J. **590**, 636 (2003).
[60] S. Nesseris and L. Perivolaropoulos, Phys. Rev. D **77**, 023504 (2008).
[61] E. V. Linder and R. N. Cahn, Astropart. Phys. **28**, 481 (2007).
[62] R. Gannouji and D. Polarski, J. Cosmol. Astropart. Phys. 05 (2008) 018.
[63] C. R. Mullis, P. Rosati, G. Lamer, H. Böehringer, A. Schwope, P. Schuecker, and R. Fassbender, Astrophys. J. **623**, L85 (2005); S. A. Stanford *et al.*, Astrophys. J. **646**, L13 (2006).
[64] J. E. Gunn and J. R. Gott, Astrophys. J. **176**, 1 (1972).
[65] D. F. Mota and C. van de Bruck, Astron. Astrophys. **421**, 71 (2004).
[66] I. Maor and O. Lahav, J. Cosmol. Astropart. Phys. 7, 3 (2005).
[67] P. Wang, Astrophys. J. **640**, 18 (2006).
[68] S. Basilakos and N. Voglis, Mon. Not. R. Astron. Soc. **374**, 269 (2007).
[69] O. Lahav, P. B. Lilje, J. R. Primack, and M. J. Rees, Mon. Not. Astron. Soc. **251**, 128 (1991).
[70] C. Horellou and J. Berge, Mon. Not. R. Astron. Soc. **360**, 1393 (2005).
[71] W. J. Percival, Astron. Astrophys. **443**, 819 (2005).